Hindawi
International Journal of Chemical Engineering
Volume 2023, Article ID 8378162, 12 pages
https://doi.org/10.1155/2023/8378162

Research Article

Regeneration Analysis of Bone Char Used in Water Defluoridation: Chemical Desorption Route, Surface Chemistry Analysis and Modeling

Herson Antonio González-Ponce,[1,2] **Didilia Ileana Mendoza-Castillo**,[1,3] **Adrián Bonilla-Petriciolet**,[1] **Hilda Elizabeth Reynel-Ávila**,[1,3] **and Karla Iveth Camacho-Aguilar**[1]

[1]*Instituto Tecnológico de Aguascalientes, Aguascalientes 20256, Mexico*
[2]*Centro de Bachillerato Tecnológico Industrial y de Servicios No. 168, Dirección General de Educación Tecnológica Industrial, Aguascalientes 20010, Mexico*
[3]*CONACyT, Ciudad de México 03940, Mexico*

Correspondence should be addressed to Herson Antonio González-Ponce; herson_qfbd@hotmail.com

Received 26 October 2022; Revised 23 February 2023; Accepted 25 February 2023; Published 6 March 2023

Academic Editor: Sebastien Déon

High concentrations of fluoride (F^-) in drinking water represent a public health threat, and consequently, effective and sustainable methods are required to improve the water quality, mainly in developing and low-income countries. This study focused on the thermodynamics of fluoride adsorption on bone char regenerated with NaOH for water defluoridation. A detailed analysis of the number of fluoride adsorption/desorption cycles, their impact on the performance and surface chemistry of bone char using different NaOH concentrations, and modeling of the adsorption mechanism using statistical physics theory was carried out. The results showed that 0.075 mol/L NaOH was effective in recuperating the defluoridation properties of bone char with a regeneration efficiency higher than 90% during five adsorption/desorption cycles. Bone char regeneration efficiency decreased up to 64% after ten adsorption/desorption cycles with a maximum fluoride adsorption capacity of 0.18 mmol/g. NaOH restored the bone char surface properties for ligand exchange of the fluoride anions via the hydroxyapatite functionalities contained in this adsorbent. It was calculated that around 0.25–0.46 mmol/g hydroxyapatite ligand exchange sites of regenerated bone char samples could be involved in the fluoride adsorption, which was also expected to be a mono-ligand mechanism. The reduction in defluoridation properties of bone char during the regeneration cycles was attributed to the decrease in the ligand exchange capacity as well as the deactivation and blocking of some functional groups of hydroxyapatite, which limited their participation in consecutive adsorption processes. This study contributes to the optimization of the recycling and reuse of bone char for fluoride removal from water to reduce the operating defluoridation costs, thus enhancing the application of this technology in low-income areas where fluorinated water represents a threat to public health.

1. Introduction

In the earth, fluoride (F^-) is a halogen widely distributed and commonly present in trace amounts in soil, groundwater, and air [1]. The presence of fluoride in the environment is related to the dissolution of minerals from rocks, aerosols from seawater, volcanic emissions, and anthropogenic activities [2, 3]. Currently, humans are exposed to fluoride directly or indirectly via their diet, personal care and hygiene products, pharmaceuticals, tobacco consumption, fluoride-containing drugs, and environmental pollution of water, soil, and air [4, 5]. However, chronic exposure to high fluoride concentrations, mainly via drinking water consumption, has been reported to cause side effects such as fluorosis in calcified tissues (bones and teeth) and the incidence of chronic degenerative diseases in soft tissues such

as liver, kidneys, heart, and central nervous system [5]. The incidence of fluoride-related diseases in populations from different countries has increased in recent decades owing to the difficulty in accessing clean and purified drinking water in developing countries [6]. Therefore, the World Health Organization (WHO) has established a guideline value of fluoride in drinking water at a maximum of 1.5 mg/L to minimize fluoride exposure toxicity [7].

There are different techniques to remove fluoride from aqueous solutions and reduce the exposure of the population to this toxic water pollutant; however, not all alternatives are optimal due to their cost-effectiveness and environmental impact. The selection of the best technology for the removal of specific target pollutants relies on selectivity, cost-effectiveness, energy consumption, and environmental impact. Adsorption is a viable and reliable technology for wastewater and groundwater treatment and purification. This process is flexible, versatile, requires low energy, and can be applied in real life for water sanitation [8]. Activated carbon is a universal adsorbent that is used for the removal of organic and inorganic water pollutants [9]. Novel adsorbents have been introduced to remove different water pollutants, and special attention has been paid to tailoring their surface functionalities and textural parameters [10–12]. However, there is a growing interest in the use of alternative adsorbents for water treatment that can be prepared from agricultural by-products and nontraditional biomass [13–18]. These alternative adsorbents are characterized by their low cost, competitive adsorption capacity, and reduced environmental pollution.

On the other hand, the reduction, recycling, and correct disposal of municipal solid wastes also represent an important improvement in environmental quality that clearly contributes to human health protection. It has been estimated that solid waste generation in 2025 will be approximately 2.2 billion tons, which could be linked to serious health problems around the world [19]. A significant amount of solid waste in industrialized countries is generated by food, with ~222 million tons globally [20]. Only in the U.S., the total food waste disposed per year was estimated at 35.5 million tons in 2015 [21]. The amount of food waste, including meat and bone residues, continues to increase annually. It is estimated that they will increase globally in the next decade by 16% for beef and veal meat, 21% for sheep meat, 18% for poultry, and 11% for pig meat [22]. The disposal of bone residues also represents a human health problem due to the presence of pathogens. Alternatives to reduce and recycle these bone wastes are required to minimize environmental impact and population health risks. The application of pyrolysis of bone waste offers the possibility of generating value-added products such as bone char [23].

Bone char (BC) is considered an eco-friendly material because of its low-cost, biocompatibility, and contribution to the sustainable recycling of bone wastes [24]. The major component of BC is hydroxyapatite, which accounts for approximately 70–80% of its total content. The composition of calcium hydroxyapatite makes it an interesting material for biological and chemical processes due to its ion exchange properties [25, 26]. BC has also been recognized as the best commercial adsorbent already available in different countries for facing water defluoridation. After the use of BC for fluoride adsorption, it is important to recycle and dispose of it properly. Despite the benefits of BC production, its life cycle and regeneration chemistry as an adsorbent for fluoride removal have not been analyzed in detail. To date, thermal and chemical-based methods for BC regeneration have been tested and reported [27–29]. Chemical regeneration is a common approach for the desorption of pollutants from adsorbent surfaces and is characterized by its low energy requirement and high regeneration efficiency [30]. The results of some studies have shown that the chemical regeneration with sodium hydroxide (NaOH) offers additional advantages in terms of energy consumption and process efficacy to recover the defluoridation properties of this adsorbent. Consequently, the analysis and optimization of BC regeneration with NaOH are fundamental for reducing the operating costs of fluoride removal and developing effective methods for water treatment.

The aim of this study was to analyze the thermodynamics and surface chemistry of the regeneration of BC used in water defluoridation. This information is relevant to improve the application of this adsorbent as an effective separation medium to reduce the fluoride concentrations in polluted drinking water, thus generating its corresponding benefits in terms of human health and environmental protection. A detailed analysis of the number of cycles in that BC can be regenerated and reused for fluoride removal is reported. BC regeneration was carried out with NaOH, and a detailed physicochemical characterization of the reused adsorbent was also performed. Theoretical calculations from statistical physics were employed to understand the impact of NaOH regeneration on the adsorbent surface chemistry.

2. Methodology

2.1. Materials and Reagents. Commercial BC was obtained from Bonechar Carvão Ativado®, Paraná, Brazil. Sodium hydroxide (NaOH) was purchased from Karal®, Mexico. Sodium fluoride (NaF) was purchased from J. T. Baker®, Mexico, while the fluoride adjustment buffer powder pillows were obtained from Hach®, USA. Deionized water was used in all experiments.

2.2. Fluoride Adsorption and Desorption Studies Using BC. The adsorption and desorption of fluoride on BC were analyzed under batch operating conditions. Fluoride desorption kinetics and adsorption isotherms of regenerated BC were quantified. First, BC samples were saturated with fluoride solutions of different initial concentrations ($[F^-]_i$), ranging from 1 to 13 mmol/L, at pH 7 and 30°C using a water bath under continuous stirring (120 rpm) for 48 h with a ratio of 2 g of adsorbent (m) per 1 L of fluoride solution (V). Preliminary studies confirmed that this operating time was sufficient to reach the adsorption equilibrium and to achieve the adsorbent saturation. The maximum adsorption capacities of BC after different

regeneration cycles were obtained from these isotherms. Fluoride adsorption capacities (q, mmol/g) of raw and regenerated BC samples were determined with the corresponding material balance.

$$q = \left(\frac{[F^-]_i - [F^-]_e}{m}\right) \bullet V, \tag{1}$$

where $[F^-]_e$ is the equilibrium fluoride concentration in the aqueous solution (mmol/L).

In the second stage, BC samples saturated with the highest fluoride concentration were used in desorption studies. Fluoride desorption kinetics were carried out with NaOH concentrations of 0.01, 0.05, and 0.075 mol/L. These desorption studies were performed in a water bath at 30°C under continuous stirring (120 rpm) with 2 g of fluoride-saturated BC per 1 L of NaOH solution. The fluoride concentration profile in the NaOH solution due to the desorption was monitored for 48 h. BC regenerated with NaOH was washed with deionized water, dried, and used in the next adsorption cycle to determine the corresponding adsorption isotherm and quantify its maximum adsorption capacity after regeneration. Ten fluoride adsorption-desorption cycles were performed to analyze the defluoridation properties and surface chemistry of the regenerated adsorbent.

The desorption efficiency (DE, %) and regeneration efficiency (RE, %) were calculated to study and compare the fluoride adsorption properties of regenerated BC samples after different adsorption/desorption cycles under the same operating conditions. DE and RE were calculated with the equations [30]

$$\begin{aligned} \mathrm{DE} &= \left(\frac{m_{F,\mathrm{NaOH}}}{m_{F,BC}}\right) \bullet 100, \\ \mathrm{RE} &= \left(\frac{q_{reg}}{q_{raw}}\right) \bullet 100, \end{aligned} \tag{2}$$

where $m_{\mathrm{F,BC}}$ (mmol) is the amount of fluoride adsorbed on BC before the NaOH regeneration, $m_{\mathrm{F,NaOH}}$ (mmol) is the amount of fluoride desorbed with NaOH during the regeneration step, q_{reg} is the fluoride adsorption capacity (mmol/g) of the regenerated BC at different adsorption-desorption cycles, and q_{raw} is the fluoride adsorption capacity of raw BC (mmol/g), respectively.

The fluoride concentrations in the aqueous solutions obtained from the adsorption and regeneration experiments were quantified using a selective electrode. Fluoride quantification was performed at 30°C with a buffered solution via powder pillows following the method reported by Rojas-Mayorga et al. [31]. Standard curves were obtained with fluoride solutions where a logarithmic curve ($\log_{10}$) was employed to obtain a linear regression of millivolts (mV) versus fluoride concentration with $R^2 > 0.9$. One-way ANOVA with a multiple comparison post-test (Tukey) and a confidence level of 95% was performed for the data analysis using the software GraphPad Prism 8.

2.3. Surface Chemistry Characterization of Regenerated BC. Fourier transform infrared (FTIR) spectroscopy was used to characterize the surface functional groups of raw and regenerated adsorbent samples. KBr powder and BC were mixed and pressed to form the KBr pellets, which were analyzed in the wavenumber range of 400–4000 cm^{-1} at room temperature with a resolution of 4 cm^{-1} using a Nicolet iS10 FTIR Thermo Scientific spectrometer. X-ray diffraction (XRD) patterns were recorded to assess the crystallographic changes on the surface of regenerated BC. An Empyrean X-ray diffractometer was employed in the sample analysis, which was carried out at room temperature with a PIXcel1D-Medipix3 detector and CuKα radiation ($\lambda = 1.5406$ Å, 45 kV, 40 mA) in the angle range from 20 to 70° 2θ. The amounts of calcium and phosphate oxides in BC samples were quantified via X-ray fluorescence, and these compositions were correlated with possible structural changes in the regenerated adsorbent. This determination was carried out by preparing glass disks by lithium borate fusion and using a 3-kW sequential XRF spectrometer Zetium Panalytical in a vacuum system with Ar/CH_4 flow. N_2 adsorption-desorption at −196.15°C was utilized to determine the textural properties (BET surface area, pore volume, and size) of the regenerated BC samples where an ASAP 2020 Micrometrics instrument was used. Morphological characteristics and elemental composition of raw and regenerated BC were studied by SEM/EDX analysis performed with a Hitachi (TM3000) scanning electron microscope and an energy dispersion system (Nano XFlash) coupled with SEM, respectively.

2.4. Calculation of Physicochemical Parameters of Fluoride Adsorption on Regenerated BC. A monolayer adsorption model based on statistical physics [32] was used to calculate the steric physicochemical parameters of fluoride adsorption on regenerated BC. This model is defined as follows:

$$q = \frac{n_F D_{BC}}{1 + \left([F^-]_{1/2}/[F^-]_e\right)^{n_F}}, \tag{3}$$

where n_{F} is the steric parameter associated with the number of fluoride ions adsorbed per binding site of BC, D_{BC} (mmol/g) is the concentration of functional groups on BC surface involved in the fluoride adsorption, and $[F^-]_{1/2}$ (mmol/L) is the fluoride concentration at the half saturation. The parameters of this adsorption model were calculated from the correlation of adsorption isotherms of the raw and regenerated bone char samples. A simultaneous nonlinear regression of all experimental adsorption isotherms was performed using an artificial neural network to calculate the best model parameters following the procedure reported by Rodríguez–Romero et al. [33]. A feed-forward artificial neural network with one hidden layer and one hidden neuron was employed in data modeling, where the input variables were the fluoride equilibrium concentrations and the number of regeneration cycles, while the output variables were the parameters of this statistical physics model, as shown in Figure 1(a). This data modeling was applied to the results for each NaOH concentration. Fluoride desorption

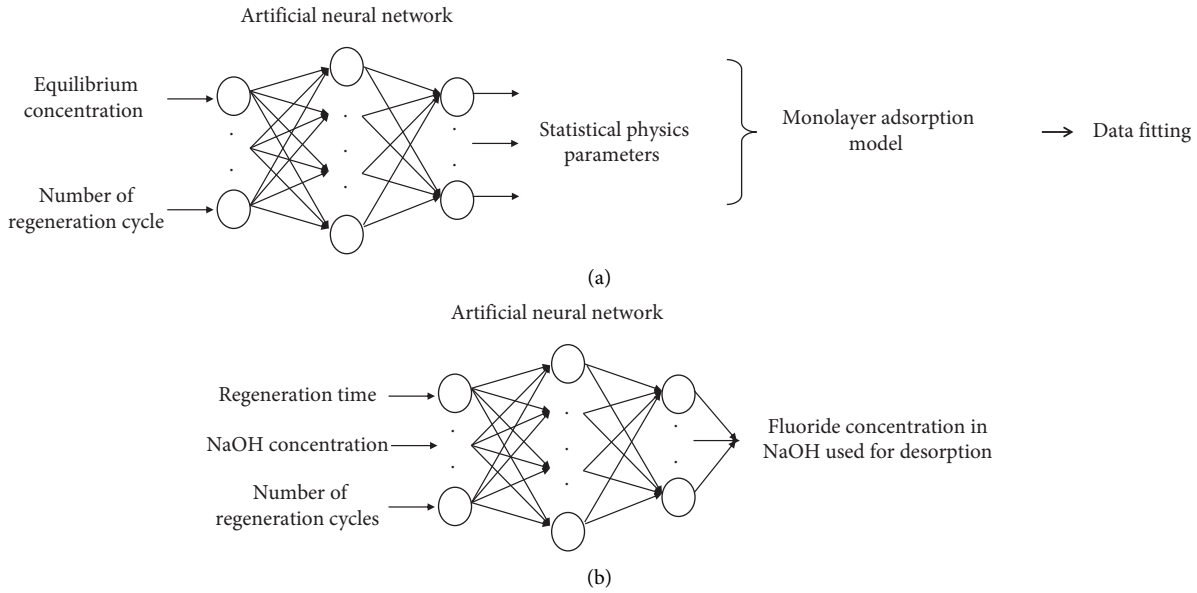

Figure 1: Illustration of ANNs-based approach to model (a) fluoride isotherms of regenerated bone char and (b) fluoride desorption kinetics in NaOH solution.

kinetics were also modeled with an artificial neural network where the input variables were the regeneration time, NaOH concentration, and the number of regeneration cycles, see Figure 1(b).

3. Results and Discussion

3.1. Defluoridation Adsorption Properties of Regenerated BC. Fluoride desorption kinetics of BC for tested NaOH concentrations are reported in Figure 2. Overall, the amount of fluoride desorbed from the BC surface increased with NaOH concentration during the regeneration. For example, the desorbed fluoride increased by 22% when the NaOH concentration changed from 0.01 to 0.05 mol/L and 9% from 0.05 to 0.075 mol/L. This trend was observed for all regenerated BC samples independent of the number of regeneration cycles. However, the NaOH effectiveness for the desorption of fluoride anions from the BC surface was reduced as more adsorption-desorption cycles were performed. DE of NaOH ranged from 53 to 76% and increased with respect to NaOH concentration. In particular, the fluoride desorption efficiencies (DE) were 53 – 59, 65 – 70, and 69 – 76% with 0.01, 0.05, and 0.075 mol/L NaOH solutions, respectively. This parameter also decreased as the number of regeneration cycles increased, indicating that the NaOH was less effective for the desorption of fluoride ions from the BC surface. These findings confirmed the role of NaOH concentration in the recovery of the fluoride ions from spent BC. Kinetic results also showed that 48 h was sufficient to reach the desorption equilibrium where the amount of fluoride anions desorbed from the BC surface was the maximum. Desorption studies for a wide variety of adsorbates and adsorbents have concluded that there is a minimum concentration of the desorbing chemical required to obtain an acceptable adsorbent regeneration [30]. NaOH concentration of 0.075 mol/L appears to be effective for the regeneration of BC employed in water defluoridation at tested experimental conditions. This NaOH concentration was significantly lower than that used in other regeneration studies of BC for water defluoridation, where NaOH concentrations up to 0.5 mol/L have been reported [28, 34]. Therefore, the application of this low NaOH concentration can contribute to the minimization of the regeneration costs of this adsorbent.

The modeling of fluoride desorption kinetics with the artificial neural network ($R^2 > 0.95$) is reported in Figure 2. This surrogate model was effective in correlating the fluoride desorption profiles of BC regenerated with NaOH solution. Fluoride desorption rate constants of BC were also calculated from these concentration profiles using the next expression.

$$[F^-]_{t,\mathrm{NaOH}} = [F^-]_{e,\mathrm{NaOH}}\left(1 - \exp^{-tk_{\mathrm{des}}}\right), \tag{4}$$

where $[\mathrm{F}^-]_{t,\mathrm{NaOH}}$ and $[\mathrm{F}^-]_{e,\mathrm{NaOH}}$ are the fluoride concentrations (mmol/L) at time t (h) and the equilibrium of the NaOH solution during the BC regeneration, and k_{des} is the fluoride desorption rate constant (h^{-1}). Calculated fluoride desorption rate constants ranged from 0.27 to 0.87 h^{-1}. It was identified that k_{des} values for fluoride desorption with 0.075 mol/L NaOH were higher than those obtained for 0.05 and 0.01 mol/L NaOH in all regeneration cycles. Moreover, the fluoride desorption rate decreased as the number of adsorption-desorption cycles increased. These results confirmed that the NaOH desorption efficiency diminished as BC was regenerated several times. After each regeneration cycle, the BC surface functionalities lost their ability to interact with and bind to fluoride ions during the adsorption.

Fluoride adsorption isotherms for raw and regenerated BC samples with different NaOH concentrations are reported in Figure 3. Raw BC showed a maximum adsorption

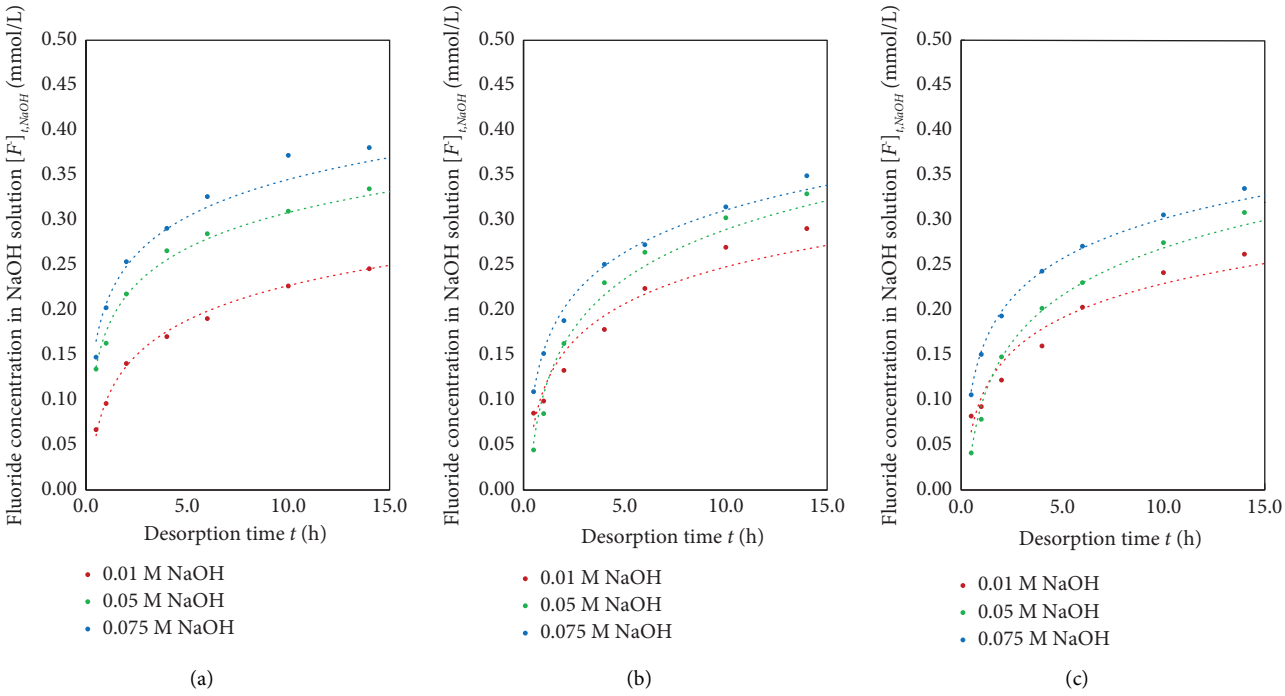

FIGURE 2: Fluoride desorption kinetics of bone char using NaOH solution at pH 7 and 30°C. (a) 1st regeneration. (b) 5th regeneration. (c) 10th regeneration.

capacity of 0.28 mmol/g at pH 7 and 30°C, while the maximum experimental adsorption capacities of regenerated adsorbents (for a maximum of 10 adsorption/desorption cycles) ranged from 0.11 to 0.21 mmol/g for 0.01 mol/L NaOH, 0.13 to 0.25 mmol/g for 0.05 mol/L NaOH, and 0.18 to 0.26 mmol/g for 0.075 mol/L NaOH, respectively. These results indicated a significant decrease ($p < 0.05$) of the defluoridation properties of BC regenerated with 0.01 mol/L NaOH at the 1st, 5th, and 10th adsorption/desorption cycles (i.e., 23, 58, and 62%) in comparison to the raw BC. In the case of adsorbent samples regenerated with 0.05 mol/L NaOH, their fluoride adsorption capacity decreased from 9 to 53% ($p < 0.05$) during the adsorption-desorption cycle. BC samples regenerated with 0.075 mol/L NaOH showed the lowest decrease in their adsorption capacities during the first 5 adsorption/desorption cycles (i.e., 4–16%), but their defluoridation performance decreased significantly at the 10th regeneration cycle (36%) with respect to raw BC. ANOVA confirmed that these differences were statistically significant ($p < 0.05$).

Overall, RE values were 38–77, 47–91, and 64–96% for the adsorbent regeneration with NaOH concentrations of 0.01, 0.05, and 0.075 mol/L, respectively, as shown in Figure 4. The fluoride adsorption capacity of BC regenerated with a concentration of 0.01 mol/L of NaOH was considerably reduced after the first adsorption/desorption cycle (RE = 77%). After 10 regeneration cycles using 0.01 mol/L NaOH, this adsorbent showed the lowest fluoride adsorption capacity, which was reduced by more than 62% with respect to the raw BC. NaOH concentrations of 0.05 and 0.075 mol/L were more effective for recovering the defluoridation properties of BC during several adsorption-desorption cycles. However, 0.075 mol/L NaOH was the best concentration to desorb fluoride anions and regenerate spent BC with RE of 64–96%. In fact, this NaOH concentration was very effective for the BC regeneration during early adsorption-desorption cycles where the fluoride adsorption properties were successfully recovered with RE >90%. These findings were consistent with the results of previous studies (e.g., [28, 34]. For instance, Nigri et al. [28] regenerated BC used for fluoride removal on a fixed-bed column using 0.5 mol/L NaOH. These authors concluded that the BC adsorption capacity decreased by 70% with RE = 30% for 5th regeneration cycle. But it is convenient to recall that these authors used a higher NaOH concentration in the BC regeneration studies. This comparison clearly highlights the importance of identifying the best concentration of the desorbing agent to improve the adsorbent properties and to reduce the regeneration costs. NaOH concentration is a paramount parameter that must be taken into consideration to obtain the highest values of regeneration effectiveness. The results point out that very low NaOH concentrations might not be enough for the desorption of fluoride anions loaded on the BC surface, thus affecting the recovery of its adsorption properties. In contrast, a high NaOH concentration could reduce the regeneration effectiveness, affecting the adsorbent performance by the inactivation or damage of the adsorbent functional groups. NaOH-based regeneration was also more effective than the BC thermal regeneration for fluoride removal. The results reported by Nigri et al. [29] indicated that 55% RE of BC can be achieved in the 1st adsorption-desorption cycle with thermal regeneration at 400°C thus proving that this approach was less reliable and implied a major cost due to the

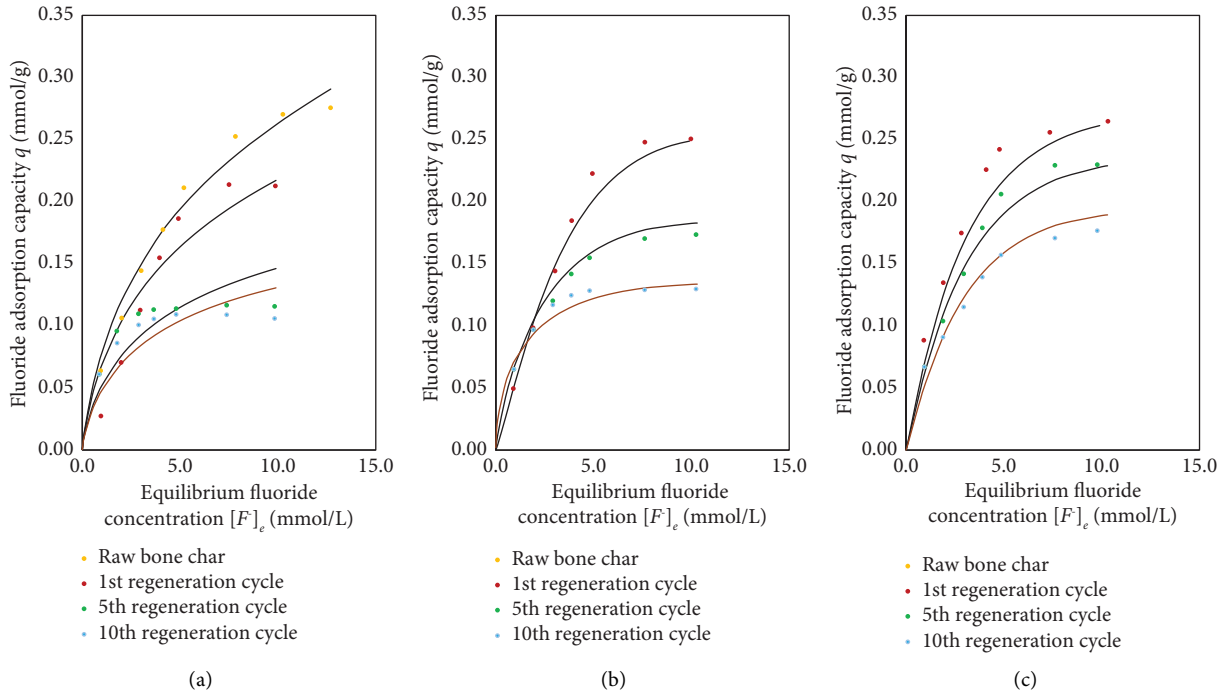

Figure 3: Fluoride adsorption isotherms using raw and regenerated bone char samples at pH 7 and 30°C. (a) Regeneration with 0.01 M NaOH. (b) Regeneration with 0.05 M NaOH. (c) Regeneration with 0.075 M NaOH.

energy consumption in the adsorbent thermal treatment. Moreover, it is convenient to indicate that the fluoride adsorption properties of regenerated bone char can be competitive with respect to other adsorbents reported in the literature; see Table 1.

3.2. Surface Chemistry and Characterization of Regenerated Bone Char with NaOH. In general, the defluoridation properties of BC are related to the content of hydroxyapatite in the adsorbent structure [25, 26, 35, 36]. Previous studies have shown that the preparation conditions of BC significantly affect its fluoride adsorption capacity, where the pyrolysis or carbonization temperature plays a relevant role [24, 31, 35]. Figueiredo et al. [37] reported that the presence of hydroxyapatite in BC samples is dependent on the calcination temperature. Mammalian bones are composed of nanocrystalline apatite and fibrous protein. The organic matter (mainly collagen) of this biomass can undergo combustion at 200–600°C, which is completed at approximately 650°C, thus leading to the formation of porous hydroxyapatite at 700°C [38, 39]. Note that the combustion of collagen at >400°C affects the crystallite size and the degree of crystallinity of the final solid [38]. The growth of crystallite size is significant at 400–700°C and remains stable at >800°C, unlike crystallinity, which increases with temperature [38], where the hydroxyapatite structure can be preserved even at 1000°C [39, 40]. On the other hand, Rojas-Mayorga et al. [35] showed that bone pyrolysis at 700°C was the best condition to prepare BC for fluoride removal from water, thus avoiding the hydroxyapatite dehydroxylation, which has a significant impact on BC defluoridation properties.

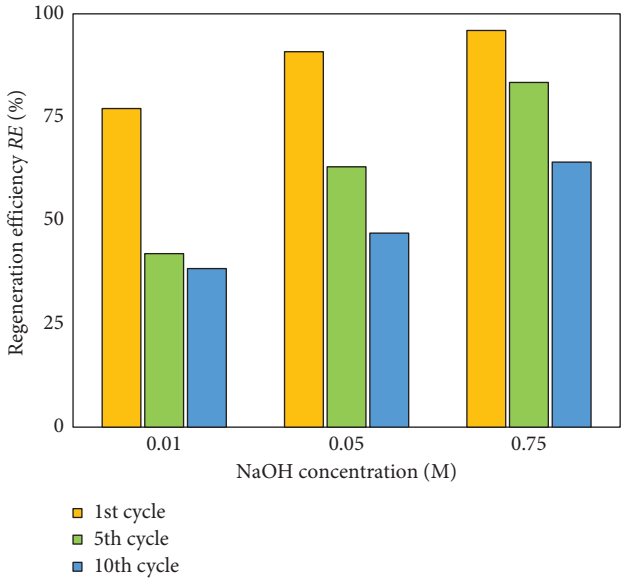

Figure 4: Regeneration efficiency of bone char using NaOH solutions.

Based on these results, the changes in the fluoride adsorption properties of regenerated BC samples are mainly associated with the impact of NaOH on the hydroxyapatite phase contained in this adsorbent, as discussed below.

The results of FTIR analysis for raw and regenerated (1st, 5th, and 10th cycles, 0.075 mol/L NaOH) BC samples are reported in Figure 5. The characteristic absorption bands of BC samples resulting from the stretching and symmetric bending modes of vibration of O-H, stretching vibration of

Table 1: Comparison of the fluoride adsorption capacities reported for commercial bone chars and other adsorbents. Adapted from Elvir-Padilla et al. [25].

Adsorbent	pH	T (°C)	q (mmol/g)
Regenerated commercial bone char	—	—	0.03
Commercial bone char	7	20–30	0.12–0.39
Cerium modified bone char	7	30	0.72
Aluminum hydroxide-coated zeolite from coal fly ash	6.0	25	0.95
Pinus roxburghii wood biochar	4.5	30	0.88

C-H, asymmetric stretching and bending vibrations of C-O from the carbonate group, and symmetric stretching and bending vibrations of P-O from the phosphate group were identified at ~3440, 2950–2850, 1620, 1450–1400, 1100–960, and 605–560 cm^{-1} [31, 41–43]. An increase in the absorption band was observed at 2013 cm^{-1} (which was associated with the presence of PO_4^{3-}) for the BC samples obtained from the 5th and 10th regeneration cycles in comparison with the raw BC, and a gradual decrease in the absorption band at 3444 cm^{-1} (associated with the presence of hydroxyl groups) of the BC samples from the 1st, 5th, and 10th regeneration cycles. After fluoride adsorption, a slight widening, and small displacement to lower frequencies were detected in the absorption band located at ~3440 cm^{-1}, which was indicative of BC surface fluoridation. Similar findings were reported by Eslami et al. [44]; Nigri et al. [29]; Shaltout et al. [45]; and Sundaram et al. [46]. These results were consistent with the expected mechanism for fluoride adsorption, where the reduction of hydroxyl groups affected the ligand exchange capability of regenerated BC samples, thus reducing their fluoride adsorption capacity in the regeneration cycle.

XRD results of raw and regenerated BC samples were similar, where the characteristic peaks were located at ~21.8, 22.9, 25.9, 28.1, 28.9, 31.8, 32.2, 32.9, 34.1, 39.8, 42.0, 46.7, 48.1, 49.5, 50.5, 51.3, 52.1, 53.1, 55.9, 61.7, 63.0, and 64.1° 2θ; see Figure 6. These diffractograms show the crystalline pattern of hydroxyapatite (ICDD: 00-009-0432) in agreement with other studies reported in the literature [26, 31, 41, 43, 47]. Notably, NaOH regeneration did not modify the crystalline structure of BC samples [48]. On the other hand, the crystalline structure of fluorapatite (ICDD: 00-015-0876) was identified after adsorption, confirming that the BC surface was loaded with fluoride ions. XRF analysis of raw and regenerated BC samples confirmed a decrease in the amount of calcium oxide. For example, this oxide content ranged from 62.1% for raw BC to 58.2% for the regenerated adsorbent at the 10th adsorption/desorption cycle, while the content of phosphorus pentoxide increased from 19.8% to 27.9% for the same samples. Consequently, the change observed in the Ca/P ratio was attributed to the NaOH treatment. The textural parameters of BC were slightly affected by NaOH regeneration; see Table 2. In particular, the BET surface areas were 58 m^2/g for raw BC, and 53–40 m^2/g for BC regenerated in the 1st–10th cycles. The surface areas of the regenerated BC samples were reduced because NaOH may have affected the internal porous structure. In addition, the desorption efficiency decreased along the regeneration cycles causing fluoride ions not desorbed from the adsorbent surface can block some pores. Note that the reduction in the surface area could also affect the fluoride adsorption capacity of regenerated adsorbents but to a minor extent. The pore size of regenerated BC samples did not show a significant difference during the fluoride adsorption/desorption cycles, which was ~5.7 nm. Finally, the microstructure of raw and regenerated BC is reported in Figure 7. Raw adsorbent presented a rough, irregular, compact, and nonporous surface. However, NaOH regeneration gradually affected the morphology of the BC surface due to the corrosion caused by this chemical along the regeneration cycles. EDX analysis confirmed that the main constituents of BC were oxygen, calcium, and phosphate, which were associated with its hydroxyapatite content.

3.3. Analysis of Fluoride Adsorption Mechanism Using Regenerated Bone Char. Ligand exchange process and electrostatic interactions are expected to be involved in the fluoride adsorption on BC and they have been associated with the hydroxyapatite phase [26, 35, 43, 49, 50]. Electrostatic interactions were caused by the positively charge of BC at pH 7 <pH at the point of zero charge (i.e., ~8). The ligand exchange for fluoride adsorption on BC can be performed via the hydroxyapatite phase:

$$Ca_{10}(PO_4)_6(OH)_2 + 2F^- \Rightarrow Ca_{10}(PO_4)_6F_2 + 2OH^-, \quad (5)$$

where two fluoride anions can be exchanged at each hydroxyapatite ligand exchange site. Therefore, NaOH performs the dual function in BC regeneration. First, NaOH desorbed the fluoride anions bonded to the hydroxyapatite functionalities of BC, thus allowing their participation in another adsorption cycle. This desorption process can be represented as follows:

$$Ca_{10}(PO_4)_6F_2 + 2OH^- \Rightarrow Ca_{10}(PO_4)_6(OH)_2 + 2F^-. \quad (6)$$

NaOH can also contribute to the activation of other functionalities available on the BC surface that can be involved in the next adsorption cycle.

Calculations with the monolayer adsorption model indicated that the number of fluoride anions adsorbed per hydroxyapatite ligand exchange site (n_F) of raw BC was ~1.1, which was consistent with the fluoride anions that could be exchanged according to (5). After BC regeneration, the calculated n_F values were 0.74–0.79 for 0.01 mol/L NaOH, 0.52–1.03 for 0.05 mol/L NaOH, and ~1.1 for 0.075 mol/L NaOH. These results suggested that the ligand exchange capacity of the hydroxyapatite phase of regenerated BC was affected as the number of regeneration cycles increased. This

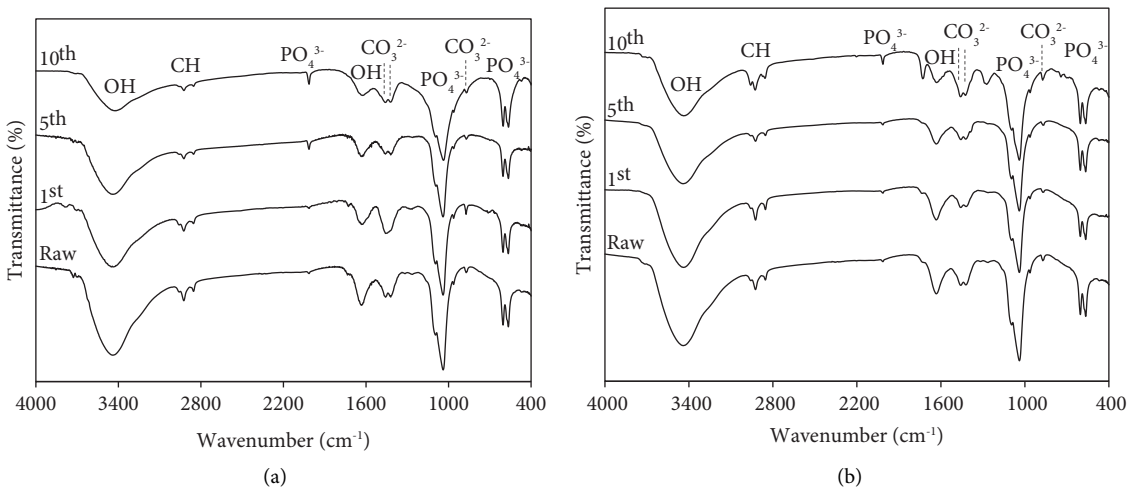

Figure 5: FTIR spectra of raw and regenerated bone chars (a) before and (b) after fluoride adsorption. Samples were regenerated with 0.075 mol/L NaOH.

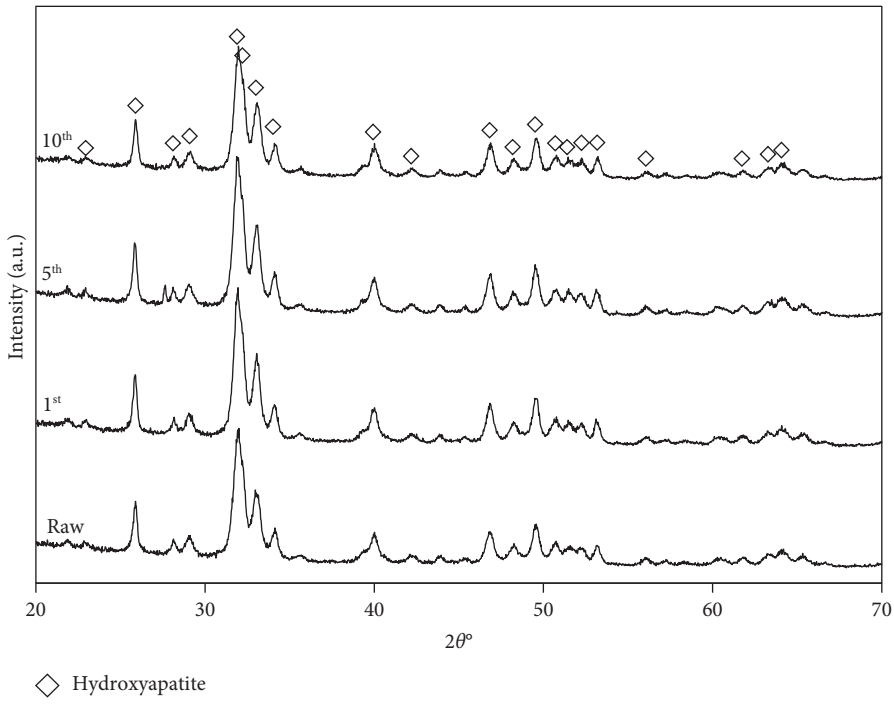

(a)

Figure 6: Continued.

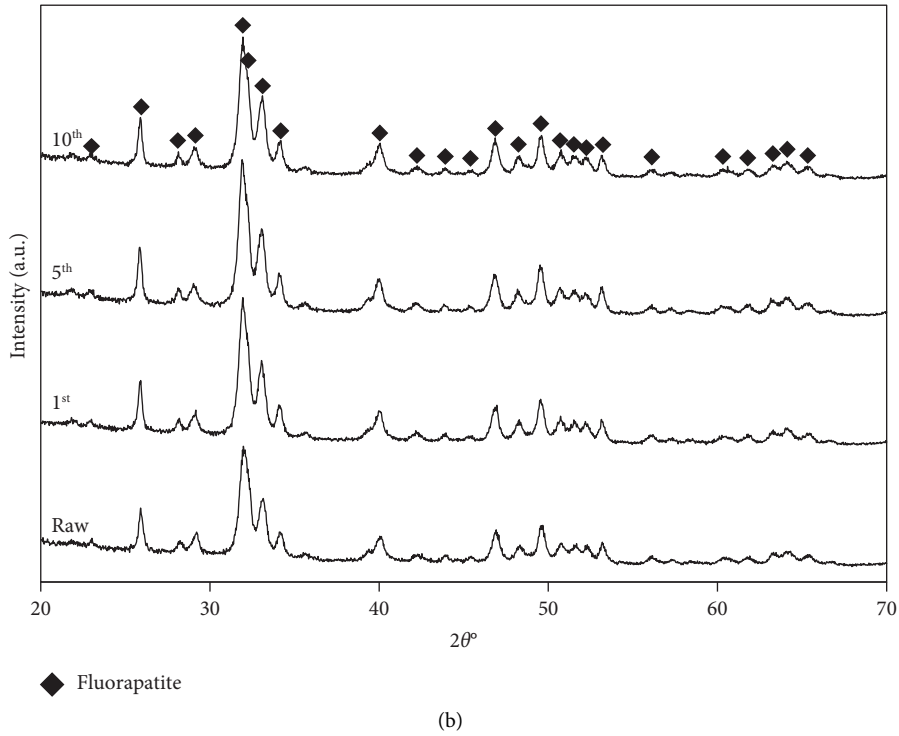

(b)

Figure 6: X-ray diffractograms of raw and regenerated bone chars (a) before and (b) after fluoride adsorption. Samples were regenerated with 0.075 mol/L NaOH.

Table 2: Textural parameters of raw and regenerated bone char samples. Samples were regenerated with 0.075 mol/L NaOH.

Sample	BET surface area (m^2/g)	Pore volume (cm^3/g)	Pore size (nm)
Raw	58	0.09	5.6
1st regeneration cycle	53	0.08	5.7
5th regeneration cycle	40	0.07	5.7
10th regeneration cycle	43	0.07	5.7

phenomenon was more noticeable at 1–5th regeneration cycles using 0.01 and 0.05 mol/L NaOH concentrations. It is interesting to highlight that the hydroxyapatite from BC samples regenerated with 0.075 mol/L NaOH maintained its ligand exchange properties (i.e., n_F of raw BC $\cong n_F$ of regenerated BC) and, consequently, they showed the highest regeneration effectiveness (i.e., RE values) at different adsorption/desorption cycles. It was also calculated that 0.47 mmol/g of hydroxyapatite ligand exchange sites (D_{BC}) were involved in the fluoride adsorption on raw BC. The quantity of these surface functionalities for fluoride adsorption was reduced after each adsorption/desorption cycle for the tested NaOH concentrations where D_{BC} ranged from 0.46–0.25 mmol/g during the 1–10th regeneration cycles. FTIR results confirmed the calculations of the monolayer adsorption model, which indicated that the number of ligand exchange sites associated with hydroxyapatite was reduced as the regeneration cycles were carried out. This finding can be associated with the deactivation of some functional groups and the incomplete fluoride desorption by NaOH, which blocked some surface functionalities for another adsorption process. Therefore, the BC regenerated with 0.075 mol/L NaOH outperformed other regenerated BC samples because their hydroxyapatite-based functional groups preserved their ligand exchange properties after several fluoride adsorption/desorption cycles. For NaOH concentrations <0.075 mol/L, the defluoridation properties of regenerated BC were affected by the functional group deactivation, the reduction of their ligand exchange properties and the inefficient fluoride desorption specially after several regeneration cycles.

Finally, the interaction energies (ΔE, kJ/mol) between fluoride anions and BC ligand exchange sites were calculated with the monolayer adsorption model via [32]

$$\Delta E = \mathrm{RTln}\left(\frac{\mathrm{Sol}_F}{[F^-]_{1/2}}\right), \tag{7}$$

where R is the universal gas constant, $\mathrm{Sol_F}$ is the solubility of fluoride in an aqueous solution (mmol/L), and T is the adsorption temperature (K) used to determine the fluoride adsorption isotherms. Fluoride–BC interaction energies

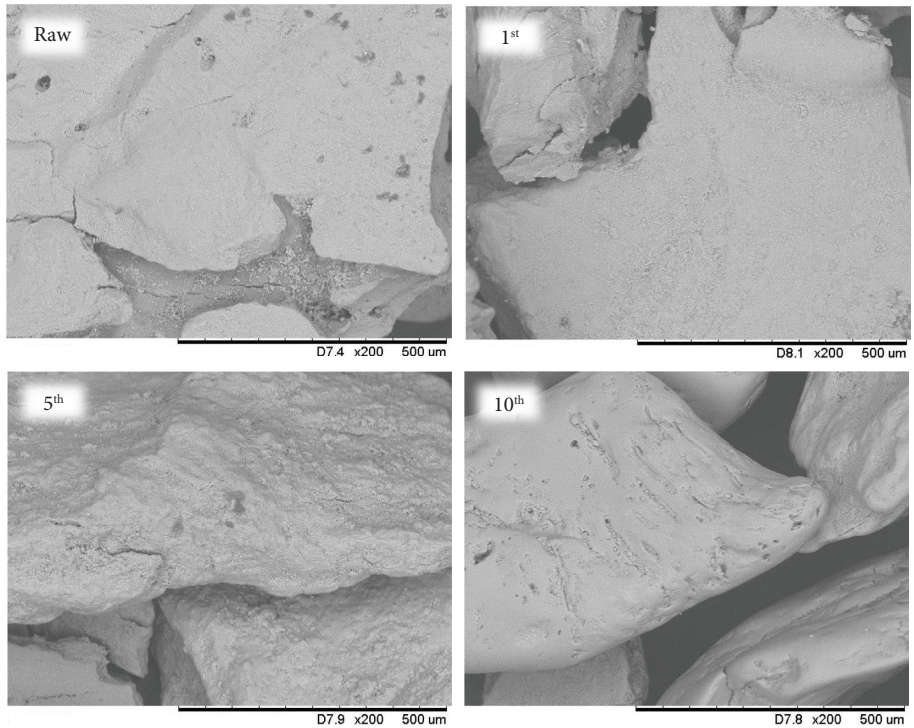

Figure 7: SEM micrographs (200x) of raw and regenerated bone chars. Samples were regenerated with 0.075 mol/L NaOH.

ranged from 12.5 to 13.9 kJ/mol and slightly increased with NaOH concentration in the regeneration cycles. These interaction energies correspond to the classical values of physical adsorption forces, which allow the adsorbate desorption and the corresponding adsorbent regeneration.

4. Conclusions

There is a need to implement new sustainable and efficient technologies for drinking water defluoridation due to the human health issues related to fluoride exposure in developing countries. The results showed that fluoride adsorption by bone char and its regeneration might represent an eco-friendly, cost-efficient, and sustainable large-scale technology to enhance environmental and human health protection. NaOH regeneration was effective in recovering the defluoridation properties of bone char. The reduction in the defluoridation properties of BC during the regeneration cycles was attributed to the decrease in the ligand exchange capacity of hydroxyapatite functionalities, in addition to the deactivation and blocking of some functional groups that limited their participation in consecutive adsorption processes. Fluorinated water is a serious health problem in developing countries, and the use of sustainable and low-cost treatment processes is mandatory. Fluoride adsorption on bone char is a reliable solution for addressing this environmental problem, and reducing its operating costs is important for extending its application to low-income populations. The regeneration of this adsorbent with NaOH can contribute to achieving this goal. Further studies are needed to determine bone char efficiency in multicomponent systems as well as its proper final disposal.

Data Availability

The data that support the findings of this study are available from the corresponding author upon reasonable request.

Conflicts of Interest

The authors declare that they have no conflicts of interest.

Authors' Contributions

All authors contributed to the study conception and design. Material preparation, data collection, and formal analysis were performed by Herson Antonio González-Ponce and Didilia-Ileana Mendoza-Castillo. Supervision was performed by Adrián Bonilla-Petriciolet. Original draft preparation was performed by Herson Antonio González-Ponce. Critical revisions and editing were performed by Didilia Ileana Mendoza-Castillo, Adrián Bonilla-Petriciolet, Hilda Elizabeth Reynel-Ávila, and Karla Iveth Camacho-Aguilar. All authors read and approved the final manuscript.

Acknowledgments

The authors would like to thank the financial support of the National Council of Science and Technology of Mexico (CONACYT) for scholarship number 710899, and I.Q. Fernando Moreno from National Cements and Concrete (CYCNA) Aguascalientes for his technical support. Herson Antonio González-Ponce has received scholarship support [No. 710899] from the National Council of Science and Technology of Mexico (CONACYT).

References

[1] D. Waugh, W. Potter, H. Limeback, and M. Godfrey, "Risk assessment of fluoride intake from tea in the republic of Ireland and its implications for public health and water fluoridation," *IJERPH*, vol. 13, no. 3, p. 259, 2016.

[2] M. T. Alarcón-Herrera, J. Bundschuh, B. Nath et al., "Co-occurrence of arsenic and fluoride in groundwater of semi-arid regions in Latin America: genesis, mobility and remediation," *Journal of Hazardous Materials*, vol. 262, pp. 960–969, 2013.

[3] N. Mumtaz, G. Pandey, and P. K. Labhasetwar, "Global fluoride occurrence, available technologies for fluoride removal, and electrolytic defluoridation: a review," *Critical Reviews in Environmental Science and Technology*, vol. 45, no. 21, pp. 2357–2389, 2015.

[4] S. Jones, B. A. Burt, P. E. Petersen, and M. A. Lennon, "The effective use of fluorides in public health," *Bulletin of the World Health Organization*, vol. 83, no. 9, pp. 670–676, 2005.

[5] G. Zhou, S. Tang, L. Yang et al., "Effects of long-term fluoride exposure on cognitive ability and the underlying mechanisms: role of autophagy and its association with apoptosis," *Toxicology and Applied Pharmacology*, vol. 378, Article ID 114608, 2019.

[6] S. J. Kashyap, R. Sankannavar, and G. M. Madhu, "Fluoride sources, toxicity and fluorosis management techniques – a brief review," *Journal of Hazardous Materials Letters*, vol. 2, Article ID 100033, 2021.

[7] World Health Organization, *Guidelines for Drinking-Water Quality*, World Health Organization, Geneva, Switzerland, 2017.

[8] M. N. Hasan, M. A. Shenashen, M. M. Hasan, H. Znad, and M. R. Awual, "Assessing of cesium removal from wastewater using functionalized wood cellulosic adsorbent," *Chemosphere*, vol. 270, Article ID 128668, 2021.

[9] A. Bhatnagar, W. Hogland, M. Marques, and M. Sillanpää, "An overview of the modification methods of activated carbon for its water treatment applications," *Chemical Engineering Journal*, vol. 219, pp. 499–511, 2013.

[10] M. R. Awual, "Efficient phosphate removal from water for controlling eutrophication using novel composite adsorbent," *Journal of Cleaner Production*, vol. 228, pp. 1311–1319, 2019.

[11] M. S. Salman, H. Znad, M. N. Hasan, and M. M. Hasan, "Optimization of innovative composite sensor for Pb(II) detection and capturing from water samples," *Microchemical Journal*, vol. 160, Article ID 105765, 2021.

[12] A. Shahat, K. T. Kubra, M. S. Salman, M. N. Hasan, and M. M. Hasan, "Novel solid-state sensor material for efficient cadmium(II) detection and capturing from wastewater," *Microchemical Journal*, vol. 164, Article ID 105967, 2021.

[13] A. Bhatnagar, M. Sillanpää, and A. Witek-Krowiak, "Agricultural waste peels as versatile biomass for water purification –a review," *Chemical Engineering Journal*, vol. 270, pp. 244–271, 2015.

[14] T. S. Hubetska, N. G. Kobylinska, and J. R. García, "Sunflower biomass power plant by-products: properties and its potential for water purification of organic pollutants," *Journal of Analytical and Applied Pyrolysis*, vol. 157, Article ID 105237, 2021.

[15] Z. Z. Ismail and H. N. AbdelKareem, "Sustainable approach for recycling waste lamb and chicken bones for fluoride removal from water followed by reusing fluoride-bearing waste in concrete," *Waste Management*, vol. 45, pp. 66–75, 2015.

[16] M. O. Thompson and J. P. Kearns, "Modeling and experimental approaches for determining fluoride diffusion kinetics in bone char sorbent and prediction of packed-bed groundwater defluoridator performance," *Water Research X*, vol. 12, Article ID 100108, 2021.

[17] O. Yılmaz and N. Tugrul, "Zinc adsorption from aqueous solution using lemon, orange, watermelon, melon, pineapple, and banana rinds," *Water Practice and Technology*, vol. 17, no. 1, pp. 318–328, 2021.

[18] M. M. Kabir, M. M. Akter, S. Khandaker et al., "Highly effective agro-waste based functional green adsorbents for toxic chromium(VI) ion removal from wastewater," *Journal of Molecular Liquids*, vol. 347, Article ID 118327, 2022.

[19] A. Singh, "Managing the uncertainty problems of municipal solid waste disposal," *Journal of Environmental Management*, vol. 240, pp. 259–265, 2019.

[20] E. Lopez-Barrera and T. Hertel, "Global food waste across the income spectrum: implications for food prices, production and resource use," *Food Policy*, vol. 98, Article ID 101874, 2021.

[21] K. L. Thyberg, D. J. Tonjes, and J. Gurevitch, "Quantification of food waste disposal in the United States: a meta-analysis," *Environmental Science and Technology*, vol. 49, no. 24, pp. 13946–13953, 2015.

[22] Oecd-Fao, *OECD-FAO Agricultural Outlook 2018-2027*, OECD Publishing, Washington, DC, USA, 2018.

[23] A. S. Giwa, F. Chang, J. Yuan, N. Ali, X. Guo, and K. Wang, "Evaluation of the potential beneficial pyrolyzed product yields from sewage sludge and bone waste disposal," *Environmental Technology & Innovation*, vol. 18, Article ID 100784, 2020.

[24] S. S. A. Alkurdi, R. A. Al-Juboori, J. Bundschuh, and I. Hamawand, "Bone char as a green sorbent for removing health threatening fluoride from drinking water," *Environment International*, vol. 127, pp. 704–719, 2019.

[25] L. G. Elvir-Padilla, D. I. Mendoza-Castillo, H. E. Reynel-Ávila, and A. Bonilla-Petriciolet, "Adsorption of dental clinic pollutants using bone char: adsorbent preparation, assessment and mechanism analysis," *Chemical Engineering Research and Design*, vol. 183, pp. 192–202, 2022.

[26] N. A. Medellin-Castillo, R. Leyva-Ramos, E. Padilla-Ortega, R. O. Perez, J. V. Flores-Cano, and M. S. Berber-Mendoza, "Adsorption capacity of bone char for removing fluoride from water solution. Role of hydroxyapatite content, adsorption mechanism and competing anions," *Journal of Industrial and Engineering Chemistry*, vol. 20, no. 6, pp. 4014–4021, 2014.

[27] M. E. Kaseva, "Optimization of regenerated bone char for fluoride removal in drinking water: a case study in Tanzania," *Journal of Water and Health*, vol. 4, no. 1, pp. 139–147, 2006.

[28] E. M. Nigri, A. L. A. Santos, A. Bhatnagar, and S. D. F. Rocha, "Chemical regeneration of bone char associated with a continuous system for defluoridation of water," *Brazilian Journal of Chemical Engineering*, vol. 36, no. 4, pp. 1631–1643, 2019.

[29] E. M. Nigri, A. Bhatnagar, and S. D. F. Rocha, "Thermal regeneration process of bone char used in the fluoride removal from aqueous solution," *Journal of Cleaner Production*, vol. 142, pp. 3558–3570, 2017.

[30] F. Salvador, N. Martin-Sanchez, R. Sanchez-Hernandez, M. J. Sanchez-Montero, and C. Izquierdo, "Regeneration of carbonaceous adsorbents. Part II: chemical, microbiological and vacuum regeneration," *Microporous and Mesoporous Materials*, vol. 202, pp. 277–296, 2015.

[31] C. K. Rojas-Mayorga, J. Silvestre-Albero, I. A. Aguayo-Villarreal, D. I. Mendoza-Castillo, and A. Bonilla-Petriciolet, "A new synthesis route for bone chars using CO2 atmosphere

and their application as fluoride adsorbents," *Microporous and Mesoporous Materials*, vol. 209, pp. 38–44, 2015.

[32] O. Amrhar, L. El Gana, and M. Mobarak, "Calculation of adsorption isotherms by statistical physics models: a review," *Environmental Chemistry Letters*, vol. 19, no. 6, pp. 4519–4547, 2021.

[33] J. A. Rodríguez-Romero, D. I. Mendoza-Castillo, H. E. Reynel-Ávila et al., "Preparation of a new adsorbent for the removal of arsenic and its simulation with artificial neural network-based adsorption models," *Journal of Environmental Chemical Engineering*, vol. 8, no. 4, Article ID 103928, 2020.

[34] K. Ak, T. K. Kinyanjui, S. M. Kariuki, and C. K. Chepkwony, "Efficiency of various sodium solutions in regeneration of fluoride saturated bone char for de-fluoridation," *IOSR Journal of Environmental Science, Toxicology and Food Technology*, vol. 8, pp. 10–16, 2014.

[35] C. K. Rojas-Mayorga, A. Bonilla-Petriciolet, I. A. Aguayo-Villarreal et al., "Optimization of pyrolysis conditions and adsorption properties of bone char for fluoride removal from water," *Journal of Analytical and Applied Pyrolysis*, vol. 104, pp. 10–18, 2013.

[36] M. K. Shahid, J. Y. Kim, G. Shin, and Y. Choi, "Effect of pyrolysis conditions on characteristics and fluoride adsorptive performance of bone char derived from bone residue," *Journal of Water Process Engineering*, vol. 37, Article ID 101499, 2020.

[37] M. Figueiredo, A. Fernando, G. Martins, J. Freitas, F. Judas, and H. Figueiredo, "Effect of the calcination temperature on the composition and microstructure of hydroxyapatite derived from human and animal bone," *Ceramics International*, vol. 36, no. 8, pp. 2383–2393, 2010.

[38] S. E. Etok, E. Valsami-Jones, T. J. Wess et al., "Structural and chemical changes of thermally treated bone apatite," *Journal of Materials Science*, vol. 42, no. 23, pp. 9807–9816, 2007.

[39] K. Haberko, M. M. Bućko, J. Brzezińska-Miecznik et al., "Natural hydroxyapatite—its behaviour during heat treatment," *Journal of the European Ceramic Society*, vol. 26, no. 4-5, pp. 537–542, 2006.

[40] C. Y. Ooi, M. Hamdi, and S. Ramesh, "Properties of hydroxyapatite produced by annealing of bovine bone," *Ceramics International*, vol. 33, no. 7, pp. 1171–1177, 2007.

[41] L. Delgadillo-Velasco, V. Hernández-Montoya, F. J. Cervantes, M. A. Montes-Morán, and D. Lira-Berlanga, "Bone char with antibacterial properties for fluoride removal: preparation, characterization and water treatment," *Journal of Environmental Management*, vol. 201, pp. 277–285, 2017.

[42] M. K. Shahid, J. Y. Kim, and Y.-G. Choi, "Synthesis of bone char from cattle bones and its application for fluoride removal from the contaminated water," *Groundwater for Sustainable Development*, vol. 8, pp. 324–331, 2019.

[43] R. Tovar-Gómez, M. R. Moreno-Virgen, J. A. Dena-Aguilar, V. Hernández-Montoya, A. Bonilla-Petriciolet, and M. A. Montes-Morán, "Modeling of fixed-bed adsorption of fluoride on bone char using a hybrid neural network approach," *Chemical Engineering Journal*, vol. 228, pp. 1098–1109, 2013.

[44] H. Eslami, M. Solati-Hashjin, and M. Tahriri, "The comparison of powder characteristics and physicochemical, mechanical and biological properties between nanostructure ceramics of hydroxyapatite and fluoridated hydroxyapatite," *Materials Science and Engineering: C*, vol. 29, no. 4, pp. 1387–1398, 2009.

[45] A. A. Shaltout, M. A. Allam, and M. A. Moharram, "FTIR spectroscopic, thermal and XRD characterization of hydroxyapatite from new natural sources," *Spectrochimica Acta Part A: Molecular and Biomolecular Spectroscopy*, vol. 83, no. 1, pp. 56–60, 2011.

[46] C. S. Sundaram, N. Viswanathan, and S. Meenakshi, "Defluoridation chemistry of synthetic hydroxyapatite at nano scale: equilibrium and kinetic studies," *Journal of Hazardous Materials*, vol. 155, no. 1-2, pp. 206–215, 2008.

[47] D. I. Mendoza-Castillo, A. Bonilla-Petriciolet, and J. Jáuregui-Rincón, "On the importance of surface chemistry and composition of Bone char for the sorption of heavy metals from aqueous solution," *Desalination and Water Treatment*, vol. 54, pp. 1651–1712, 2014.

[48] L. Chen, K.-S. Zhang, J.-Y. He, W.-H. Xu, X.-J. Huang, and J.-H. Liu, "Enhanced fluoride removal from water by sulfate-doped hydroxyapatite hierarchical hollow microspheres," *Chemical Engineering Journal*, vol. 285, pp. 616–624, 2016.

[49] X. Fan, D. J. Parker, and M. D. Smith, "Adsorption kinetics of fluoride on low cost materials," *Water Research*, vol. 37, no. 20, pp. 4929–4937, 2003.

[50] C. Sairam Sundaram, N. Viswanathan, and S. Meenakshi, "Uptake of fluoride by nano-hydroxyapatite/chitosan, a bioinorganic composite," *Bioresource Technology*, vol. 99, no. 17, pp. 8226–8230, 2008.